Relations between the Structure and Electric Conductivity of Polyaniline Protonated with Camphorsulfonic Acid

W. Łużny*,† and E. Bańka‡

Fac. of Physics & Nuclear Techn. and Fac. of Materials Science and Ceramics, University of Mining & Metallurgy, 30-059 Cracow, Poland

Received August 12, 1999; Revised Manuscript Received November 10, 1999

ABSTRACT: Polyaniline (PANI) protonated with camphorsulfonic acid (CSA) is one of the most promising conductive polymers due to its relatively high crystallinity, high electrical conductivity, and the metallic characteristics at high temperatures, i.e., a positive temperature coefficient of resistivity. The crystalline structure of this polymer system is still not known in detail; however, significant developments in this field have been achieved recently. In this work we present the results obtained for the series of 50 thin film samples of the PANI/CSA system, prepared under various conditions. These films were subjected to the X-ray diffraction study as well as electrical conductivity measurements. The results of this work clearly show that the conductivity of the samples strongly depends both on their degree of crystallinity and on the degree of order of the dopant anions. This ordering can be described quantitively by the relative intensity of properly selected diffraction reflections. Besides, some important conclusions concerning the anisotropy of the films subjected to the investigations may be drawn by comparison of the diffraction patterns obtained in a transmission and reflection geometry of diffraction.

Introduction

Polyaniline (PANI) is continuing to receive high interest in the field of conducting polymers. The electrical conductive emeraldine salt form of PANI is air stable and cheap to produce in large quantities, giving rise to many potentially possible applications.[1] This polymer has only been processable in the emeraldine base (EB) form, requiring postdoping with a protonic acid to give the emeraldine salt (ES). This route is not satisfactory, because it is difficult to achieve homogeneous doping in rather dense films. Cao et al. have shown that this problem may be solved by so-called *counterion processability*, e.g., by the processing with specific functional acids.[2] One example of the resulting polymer systems, PANI protonated with camphorsulfonic acid (CSA) and casted from *m*-cresol, has proven to be of considerable interest. Recent works have shown that this material exhibits the metallic-like characteristics at high temperatures, i.e., positive temperature coefficient of resistivity.[3] Besides, the room temperature value of its electrical conductivity is remarkably high (up to 1000 S/cm), especially for oriented samples.[4]

These very interesting properties have been intensively studied by many research groups. The results of X-ray diffraction measurements for PANI/CSA samples have been published in few papers.[4−8] Besides, some theoretical calculations concerning the molecular arrangement in the system studied have been presented.[9,10] The first models of PANI/CSA crystalline structure (as well as the results of the diffraction intensity calculations for these models) have been proposed recently.[11] The review of the research works concerning the structural properties of PANI/CSA system has been done very recently by Djurado et al.[12] The main conclusion of this work is that the structure of PANI/CSA films can be very complicated, and it strongly depends on the conditions of preparation and processing of the samples. Therefore, we have undertaken a more detailed study of the relationship between the synthesis and preparation, structure, and electrical conductivity of PANI/CSA films. Some preliminary results of this work have been already presented.[13] In the present work we report the results obtained for the series of more than 40 samples prepared in various conditions and subjected both to the X-ray diffraction measurementsand to the electrical conductivity measurements.

Experimental Section

Sample Preparation: Syntheses and Characterization. Preparation of samples investigated in this work, as well as their characteristics, has been already published with all the details by one of the authors (E. Bańka) in ref 14. Therefore, only basic information concerning sample preparation and characterization is presented here, in order that this paper is complete.

The syntheses were carried out in air, at temperatures ranging from −7 to −43 °C, in a 400 mL glass beaker cooled under steady-state conditions by immersing it either into a 4 L Dewar vessel containing an organic slush or into a jacketed outer vessel connected to a thermostat-controlled circulating chiller unit. The syntheses were performed under stirring by continuously pouring the solution of oxidant into the solution of aniline that was placed in the beaker and cooled in the ordered temperature. The oxidant solution was cooled separately at the same temperature before addition. The redox potential, the temperature, and the pH of the solution were collected point-by-point during the syntheses by a dedicated computer.

Because we tried to reproduce the so-called "standard synthesis" of MacDiarmid et al.,[21] the initial oxidant/aniline mole ratio was kept constant at 0.25. During subzero temperature syntheses, it was necessary to prevent the crystallization of any species before or at the beginning of the polymerization. The aniline molar concentration was kept within 0.39−0.42 M and the total reaction volume within 263−280 mL. The HCl molar concentration was kept within 0.51−0.53 M for the syntheses carried out at −7 and −14 °C and within 0.96−1.08 M for the syntheses carried out at lower temperatures. In these cases, 6.25 g of ammonium persulfate was dissolved in 60 mL

† Fac. of Physics & Nuclear Techn.
‡ Fac. of Materials Science and Ceramics.
* Corresponding author.

10.1021/ma9913663 CCC: $19.00 © 2000 American Chemical Society
Published on Web 01/05/2000

of 2 M HCl, and separately 10 mL of aniline was dissolved in 190 mL of a mixture of 85 or 95 mL of 3 M HCl with 95 or 85 mL of ethanol. LiCl was added in portions of $^1/_3$ and $^2/_3$ to the ammonium persulfate and aniline solutions, respectively, to the ordered molarity. In some syntheses, the oxidant at room temperature was added dropwise to the cooled aniline solution. For other syntheses, after the polymerization time of aniline to pernigraniline base (PN), a rapid reduction of PN to emeraldine hydrochloride (E.HCl) was performed by continuous addition of a solution of 3.64 g (0.0183 mol) of $FeCl_2$ in 50 mL of HCl containing 5 g of LiCl. The time of addition and the temperature of the solution of $FeCl_2$ were formerly determined from the potential and temperature profile of a previous synthesis at the same ordered temperature without reduction. In some other syntheses, polymerization accelerators (*N*-phenyl-1,4-phenylenediamine, for example) were added to the aniline solutions. The syntheses were stopped when the potential reached a constant end value. For each synthesis the suspension was then filtered through a porous glass funnel no. 4, and the green precipitate was collected, washed with copious amounts of 1 M HCl until the filtrate became colorless, and finally dried overnight at 50 °C under dynamic vacuum. The as-synthesized E.HCl was deprotonated by stirring in 1 L of 0.1 M ammonium hydroxide for 72 h. The obtained emeraldine base (EB) was then filtered, washed several times with water, and dried to constant mass at 25 °C under dynamic vacuum for 24 h.

The part of EB powder was extracted with chloroform using a Soxhlet apparatus, for the time usually between 4 and 10 h. The extracted EB was then dried at room temperature under vacuum for 5 h. Some purified EB powders were further deprotonated by stirring in 1 L of 0.3 M ammonium hydroxide for 48 h.

Using such procedures, the following sets of samples have been obtained: 17 samples obtained at various temperatures, concentration of LiCl, polymerization time, and reducer used (listed with all details in Table 1 of ref 14), nine samples obtained using different modes of addition of the oxidant or the polymerization accelerators applied (listed in Table 2 of ref 14), and 13 samples extracted with chloroform (listed in Table 3 of ref 14).

All samples were subjected to very careful characterization, using following methods: viscometry, GPC, UV−vis spectrometry, and chemical analysis. The results of all those measurements for each sample investigated are collected in Tables 1−3 of ref 14.

The solutions of EB protonated with CSA have been prepared by dissolving of 0.1 g of EB and 0.13 g of ±CSA in 19.8 mL of *m*-cresol (the molar ratio of CSA/N was equal to 0.5). Such solutions were stirred at 50 °C for 48 h and then at the room temperature for 3 weeks. The quality of solutions was checked by use of optical microscopy (in transmission) as well as UV−vis−NIR spectroscopy. In solutions selected for film preparation no polymer grains were observed. The films of PANI/CSA with a thickness of ∼20 μm have been obtained by solution coating on glass plates and evaporating of *m*-cresol at 50 °C for 3 days. The films have been taken off the glasses by wetting in 1 M solution of CSA for 1 h, and then they were washed and dried.

CSA-protonated EB samples were characterized by UV−vis−NIR spectroscopy, their room-temperature electrical conductivity was measured, and a few of them were subjected to the preliminary X-ray diffraction study.

Experiment. The X-ray diffraction experiments were carried out on a SEIFERT-FPM XRD-7 diffractometer working in typical (θ,2θ) Bragg geometry, with a Cu Kα radiation. First of all, we collected the diffraction patterns obtained for all samples in the reflection mode. These diffractograms differ remarkably; both the degree of crystallinityand the relative intensity of the crystalline reflections change significantly from sample to sample. This problem is described in detail below.

The important observation is that there is a significant difference between all the diffractograms obtained in this work and those published earlier for the PANI/CSA samples: the diffraction maximum at $2\theta \approx 9.4°$ does not occur for any of our patterns. This effect is related to the orientational phenomena, and it has been subjected to further careful study. It was proved that the films subjected to the diffraction measurements are completely in-plane isotropic. However, the results presented in the literature[4,7] suggest that the missing reflection may have quite a different orientation that the other ones. We have proved this hypothesis by diffraction experiments held in the transmission mode for selected samples. It turned out that indeed the maximum for $2\theta \approx 9.6°$ is present for all samples investigated. This point has been thoroughly checked by the independent study of Djurado,[15] and he also observed the described effect: the discussed reflection is absent in diffractograms obtained in reflection and present in diffraction patterns collected in transmission. Such remarkable anisotropy of diffractograms obtained in transmission and in reflection (for unoriented samples!) is a really new result, and it will be subjected to further, careful analysis.

Results and Discussion

All recorded diffraction patterns are typical of semicrystalline polymers. Two components of the diffracted intensity can be distinguished: the crystalline one, related to the relatively sharp, Bragg-type reflection peaks, and the amorphous one, visible as the broad and low-intensity halo. This amorphous component, including the background, may be fitted by single Lorentzian, and the crystalline component has been fitted by the sum of the appropriate number of Gaussians. The crystalline component of the diffractograms (obtained in transmission) consists of four more or less intense reflections related to the following interplanar distances: ∼18, 6.1, 4.3, and 3.5 Å. The fourth maximum shows a large relative intensity, and it is visible for all samples investigated—even for those with the lowest crystallinity. (In a few cases it is only one reflection recorded in transmission.[15])

To classify all collected diffractograms in a more quantitive way, we proposed two parameters. The first one is simply the degree of crystallinity (DC), estimated by the Hindeleh−Johnson method.[16] This method allows to estimate the DC by the ratio of the integrated crystalline component intensity to the integrated total intensity. The second parameter has been chosen as the ratio of the integral intensity of the first reflection to the fourth one (Z_1/Z_4). We decided to take into account such a relative value of this parameter instead of the absolute intensity of the first peak Z_1, to avoid counting the similar factor two times (Z_1 itself participates in the DC). Both parameters have been easily obtained for all samples investigated from the fitting procedures described above, and they may be treated as two independent parameters, quantitatively characterizing the diffraction patterns.

The results of such parametrization are as follows. All diffraction patterns can be classified into one of six main types, described in Figure 1. Two types (namely B and F) should be divided into two subtypes: B1, B2 and F1, F2, respectively. All diffractograms included into one type are almost identical; the number of samples in each group (type or subtype) changes from three (for D type) to more than 20 (for E type). The diffractograms classified into the particular groups are represent in Figure 2.

The differences between groups B1 and B2, as well as the general tendency in this row of the classification, are shown in Figure 3. One can observe that for the diffractograms classified into the B2 group the third reflection is well visible, whereas for the B1 group it is almost absent. Similar differences and tendencies are

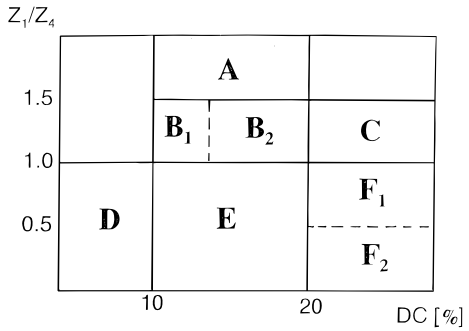

Figure 1. Diagram illustrating the classification of PANI/CSA samples with regard to their degree of crystallinity (DC) and the ratio of the integral intensity of the first diffraction reflection to the fourth one (Z_1/Z_4).

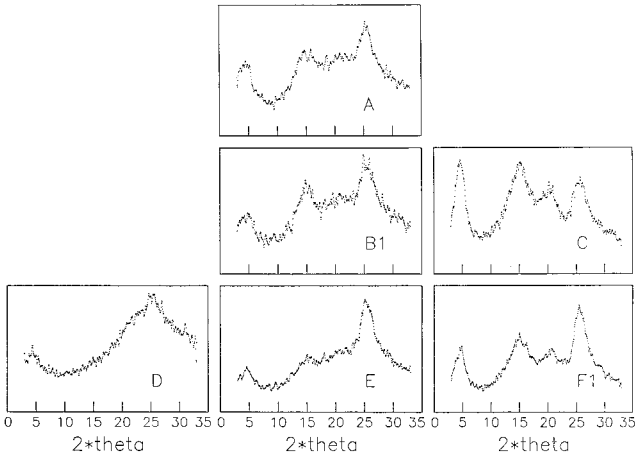

Figure 2. Diffraction patterns typical of the PANI/CSA samples classified by the particular groups defined in Figure 1.

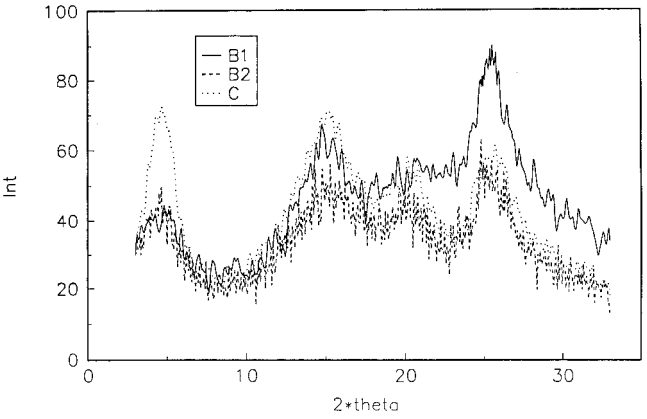

Figure 3. Diffraction patterns typical of the PANI/CSA samples classified by the groups B1, B2, and C defined in Figure 1.

shown in Figure 4, where the three types of diffractograms from the last column of the classification are well illustrated. At last, the enhancement of the first maximum relative intensity for diffraction patterns classified into the middle column is well visible in Figure 5.

As is implied from the models of the PANI/CSA structure,[11] the origin of the first diffraction maximum (for $d \approx 18$ Å) is closely related to the ordering of dopant molecules in "tunnels" between polymer chains. Contrary, the fourth reflection originates from the repetition distance between two adjacent species: a macromolecule and a dopant. Therefore, it is reasonable to conclude that the parameter Z_1/Z_4 may be treated as the measure of the ordering of CSA molecules along PANI chains: the greater the value of this parameter, the higher the ordered arrangement of these dopant anions occurs in the sample.

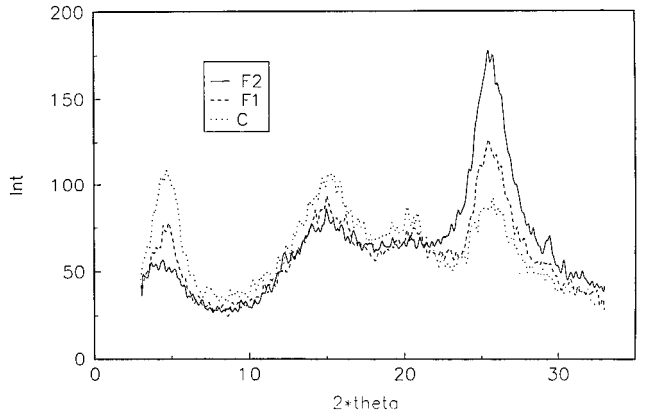

Figure 4. Diffraction patterns typical of the PANI/CSA samples classified by the groups F1, F2, and B defined in Figure 1.

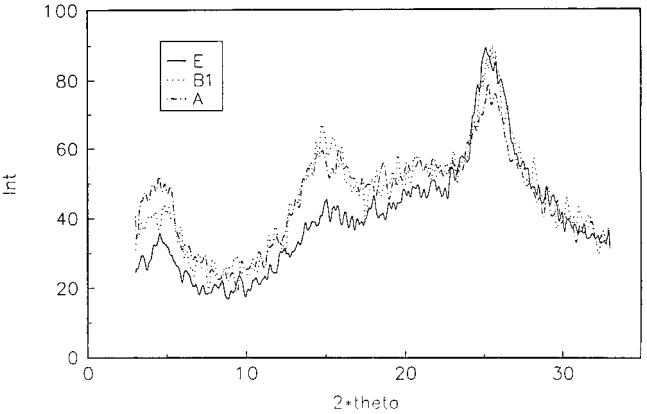

Figure 5. Diffraction patterns typical of the PANI/CSA samples classified by the groups A, B1, and E defined in Figure 1.

It is well-known that there is a strong correlation between the crystallinity of the conducting polymer sample and its electrical conductivity: the greater the degree of crystallinity, the higher the conductivity. On the other hand, the electrical conductivity inside these well-ordered regions of the polymer should be correlated to the quality of the dopants arrangement, due to the mechanism of formation of polarons and bipolarons, which are known as quasiparticles responsible for the charge transport phenomena in such a polymers as PANI. As one can notice, we obtained the unique possibility to check both these statements for the case of our long series of PANI/CSA samples, which have been classified by two parameters described above. Therefore, we calculated the average electrical conductivity for groups of samples, according to Figure 1. The results of this operation are presented in Figure 6. Without any doubt one can say that the resulting values of the conductivity are in perfect agreement with both relations explained above. The average electrical conductivity increases significantly both with increasing DC and with increasing Z_1/Z_4.

It would be very interesting now to describe the conditions of preparation and processing of the samples classified by the particular groups. Unfortunately, this cannot be done quite univocally. One can only say that

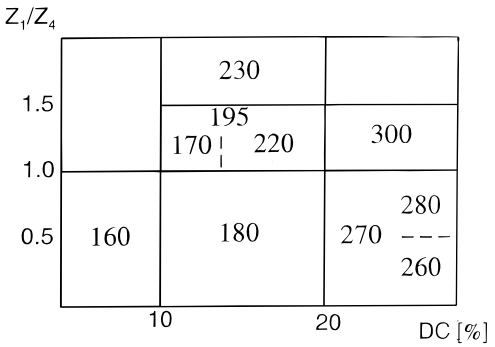

Figure 6. Average electrical conductivity [S/cm] of the PANI/CSA samples classified by the particular groups defined in Figure 1.

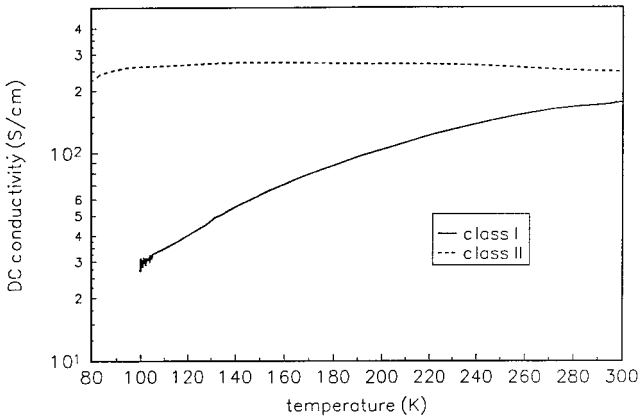

Figure 7. Temperature dependence of the electrical conductivity for two classes of the PANI/CSA samples, described in the text.

the higher conducting samples (from groups A, C,and F) have been synthesized in lower (subzero) temperatures, and in general they have greater average molar mass. Besides, the samples casted using emeraldine base extracted with chloroform show significant enhancement of their conductivity.[13]

Temperature Dependencies of the Electrical Conductivity. The relation between the electrical (dc) conductivity and the temperature of the polymer sample can give important information concerning the nature of the phenomena related to the charge transport in a polymer system. Therefore, we have undertaken such measurements for the samples of the PANI/CSA system, selected in such a way that at least one sample was chosen from each group described in Figure 1. The conductivity was measured in the range 100−300 K by use of the four-point method. The copper electrodes were used, and the set of the high-quality meters (the picoamperometer Kithley 487, for example) was connected to the PC by the GPIB card.

All traces of the dc conductivity versus the temperature recorded in this way may be easilly classified into two classes. The relations typical of both classes are shown in Figure 7.

For the first class, one can observe the temperature-activated conductivity, typical of a semiconducting material. The conductivity may increase even eight times when the temperature increases in the range investigated. The second class is characterized by the very weak dependence of the dc conductivity on the temperature. The conductivity slightly increases in the low-temperature region (ca. 80−120 K), and then it gradually decreases with the increasing temperature. The ratio of the conductivity at 300 K to its value at 120 K is close to 0.8 in these cases. Such behavior suggests the metal-like character of the conductivity in these samples, because the negative value of the thermal conductivity coefficient is related to the phonon backscattering phenomena.[3,17]

It should be underlined that the curves of the first class have been recorded for the samples from all groups described in Figure 1, whereas the curves typical of the second class have been observed only for the samples exhibiting higher conductivity, from the groups A, B, C, and F.

For the curves typical of both classes, described above, the model functions have been fitted. For the first class both Mott's formula (VRH model: variable range hopping) and Sheng's formula (FIT model: fluctuation-induced tunneling) can be applied:[18,19]

$$\sigma_M(T) = \sigma_0 \exp[-(T_0/T)^{\gamma}] \quad (1)$$

$$\sigma_S(T) = \sigma_0 \exp[-T_0/(T + T_1)] \quad (2)$$

In Sheng's model the T_1 parameter is the temperature below which only the elastic tunneling through barriers occurs, and the T_0 parameter is the temperature above which the conductivity is thermally activated.

The typical values of the parameters obtained by fitting of these two formulas to the curves of the class I are as follows: (i) for Mott's model $\gamma = 0.78$, $T_0 = 475$ K, $\sigma_0 = 727$ S/cm; (ii) for Sheng's model $T_0 = 390$ K, $T_1 = 25$ K, $\sigma_0 = 575$ S/cm. Such a high value of the γ parameter suggests that the classical VRH model for 3D systems cannot be applied ($\gamma = {}^1/_4$) for none of the samples investigated. It seems that the theory of Sheng and Klafter,[20] which describes the conductivity in inhomogeneous, granular systems ($\gamma = 0.5-1$), would explain these data better. On the other hand, the values of the parameters obtained from the fitting of Sheng's model are quite reasonable, and one can observe that both T_0 and T_1 are greater for the samples with the greater degree of crystallinity. This suggests that the degree of ordering in the sample has an impact on the range of temperatures for which the conductivity is determined by the tunneling phenomena. Besides, one can observe that the parameter σ_0 of Sheng's model is much larger for the samples described by the large value of the parameter Z_1/Z_4 (up to the values greater than 3000 S/cm for the samples from groups A and C), and one can assume that this effect is related to very high conductivity in the metal-like "islands" formed by the regions of well-ordered dopant molecules between the polymer chains.

For the second class of samples, showing quite different temperature dependence of conductivity, it was impossible to use one of the model discussed above for fitting of the experimental data. The successful fitting has been done using the following formula for the resistivity

$$\rho = AT + B[\exp(-T_0/(T_1 + T))]^{-1} \quad (3)$$

suggested for the heterogeneous materials with very high conductivity.[3] This model consist of a linear term typical of the metal-like conductivity (due to the scattering of the charge carriers on phonons) and the FIT term discussed above. The typical values of the parameters obtained from fitting are collected in Table 1.

Table 1. Parameters of Eq 3 Fitted to the Experimental Data

group of samples	A [Ω cm/K]	B [Ω cm]	T_0 [K]	T_1 [K]
A	4.8×10^{-6}	5.5×10^{-6}	11560	1640
B	6.2×10^{-6}	1.1×10^{-3}	301	93
C	4.0×10^{-6}	2.6×10^{-4}	1105	265
F	4.0×10^{-6}	2.5×10^{-3}	33	0

One can observe that T_0 and T_1 are particularly sensitive for the value of the parameter Z_1/Z_4: they are very low for the group F and very high for the group A. This effect allows us to state that this parameter (obtained from the diffraction data only) is really closely related to the electrical transport properties of the PANI/CSA samples. Besides, the parameter B is lower for better conducting samples (groups A and C) and higher for worse conducting samples (groups B and F), which is a quite reasonable conclusion.

Conclusions

The dependencies of the electrical conductivity for the PANI/CSA samples on their crystallinity and the ordering of dopant molecules have been proved by the X-ray diffraction study and by the conductivity measurements. We have shown that the relative intensity of the first diffraction peak to the fourth one is very closely related to the parameters describing the electrical transport properties of the samples. The relationships between the conditions of sample preparation and processing and the structural and transport properties of the films investigated are not quite clear, and they should be subjected to the further investigations.

It seems that the variations of relative intensities of Bragg peaks from one diffractogram to another may be explained rather in terms of different degrees of molecular ordering in the polymer system than in terms of possible anisotropy of samples implied by the preferred orientation of the crystalline regions.[12] However, this problem should be also studied in a more detailed way.

Acknowledgment. This work was financially supported by KBN Grant 3 T09B 049 14. The technical help of Dr. Tomasz Kaniowski and Mr. Paweł Armatys in the measurements of the temperature dependencies of the conductivity is greatly acknowledged.

References and Notes

(1) See for example: Proceedings of Int. Conf. on Synth. Met., Snowbird, 1996; *Synth. Met.* **1997**, *84*.
(2) Cao, Y.; Smith, P.; Heeger, A. J. *Synth. Met.* **1992**, *48*, 91.
(3) Holland, E. R.; Pomfret, S. J.; Adams, P. N.; Monkman, A. P. *J. Phys.: Condens. Matter* **1996**, *8*, 2991.
(4) Abell, L.; Adams, P. N.; Monkman, A. P. *Polymer* **1996**, *37*, 5927.
(5) Xia, Y.; Wiesinger, J. M.; MacDiarmid, A. G. *Chem. Mater.* **1995**, *7*, 443.
(6) Pouget, J. P.; Hsu, C.-H.; MacDiarmid, A. G.; Epstein, A. J. *Synth. Met.* **1995**, *69*, 119.
(7) Minto, C. D. G.; Vaughan, A. S. *Polymer* **1997**, *38*, 2683.
(8) Djurado, D.; Nicolau, Y. F.; Dalsegg, I.; Samuelsen, E. J. *Synth. Met.* **1997**, *84*, 121.
(9) Ikkala, O. T.; Pietilä, L.-O.; Ahjopalo, L.; Österholm, H.; Passiniemi, P. J. *J. Chem. Phys.* **1995**, *103*, 9855.
(10) Vikki, T.; Pietilä, L.-O.; Österholm, H.; Ahjopalo, L.; Takala, A.; Toivo, A.; Levon, K.; Passiniemi, P. J.; Ikkala, O. T. *Macromolecules* **1996**, *29*, 2945.
(11) Łużny, W.; Samuelsen, E. J.; Djurado, D.; Nicolau, Y. F. *Synth. Met.* **1997**, *90*, 19.
(12) Djurado, D.; Nicolau, Y. F.; Rannou, P.; Łużny, W.; Samuelsen, E. J.; Terech, P.; Bée, M.; Sauvajol. J. L. *Synth. Met.* **1999**, *101*, 764.
(13) Łużny, W.; Bańka, E. *Synth. Met.* **1999**, *101*, 715.
(14) Beadle, P. M.; Nicolau, Y. F.; Bańka, E.; Rannou, P.; Djurado, D. *Synth. Met.* **1998**, *95*, 29.
(15) Djurado, D., private communication, 1998.
(16) Hindeleh, A. M.; Johnson, D. J. *J. Phys. D* **1971**, *4*, 259.
(17) Joo, J.; Prigodin, N.; Min, Y. G.; MacDiarmid, A. G.; Epstein, A. J. *Phys. Rev. B* **1994**, *50*, 12226.
(18) Wang, Z. H.; Ray, A.; MacDiarmid, A. G.; Epstein, A. J. *Phys. Rev. B* **1991**, *43*, 4373.
(19) Sheng, P. *Phys. Rev. B* **1980**, *21*, 2180.
(20) Sheng, P.; Klafter, J. *Phys. Rev. B* **1983**, *27*, 2583.
(21) MacDiarmid, A. G.; Chiang, J. C.; Richter, A. F.; Somarisi, N. L. D. In Alcacer, L., Ed.; Conducting Polymers, Special Applications; Reidel: Dordrecht, 1987; p 105.

MA9913663